

Phase memory of the electronic polarization in transient nonlinear optical spectra of gallium arsenide at 2 eV

G. Böhne, T. Sure, and R. G. Ulbrich

*IV. Physikalisches Institut der Universität Göttingen, Bunsenstrasse 11-15,
D-3400 Göttingen, Federal Republic of Germany*

W. Schäfer

Höchstleistungsrechenzentrum, Kernforschungsanlage Jülich, D-5170 Jülich, Federal Republic of Germany

(Received 12 October 1989)

We present a detailed study of transient nonlinear optical spectra for the model semiconductor gallium arsenide in the canonical pump-test configuration with 2-eV incident light pulses of 70-fs duration. Starting from first principles we show that the shape of the omnipresent “spike” around zero delay time is closely connected with a transient phase memory of the driven interband transitions. The characteristic time dependence of all nonlinear pump-test spectra reflects the influence of the dominant momentum- and energy-relaxation processes on the single-particle distributions which are coupled by the pump and test pulses. The concepts discussed are of general validity for all optically excited direct-band-gap semiconductors.

I. INTRODUCTION

The classical field of light-matter interaction is the subject of renewed and considerable interest, because ultrashort (< 100 fs) and very intense ($> 10^{14}$ W/cm²) laser-light pulses are now available.¹ The interaction of such pulses with a semiconductor in the absorbing part of the optical spectrum (laser photon energy $\hbar\omega_0 > E_G$) can generate high-carrier densities up to 10^{21} cm⁻³. Coulomb scattering among free-electron-hole pairs occurs at $n \approx 10^{17}$ cm⁻³ on a 10^{-13} -s time scale.² It is, at least for higher densities, the dominating loss mechanism for single-carrier momentum [the total momentum of both single-particle distributions, $f_e(\mathbf{k})$ and $f_h(\mathbf{k})$, is conserved for carrier-carrier scattering].³ On the other hand, the cycle time T_0 for the core motion in typical semiconductors is larger than 100 fs, so that studies of optical spectra well beyond the Born-Oppenheimer approximation⁴ are now within reach; it is possible to study optical properties of “frozen-in” lattices under the extreme condition $t_{\text{pulse}} < T_0$.⁵

An important conceptual feature of such short-pulse experiments is the occurrence of a transient phase memory. The action of both driving light fields E_{pump} and E_{test} on the polarizable carriers induces a correlation of phases, which is linked to the off-diagonal terms of the corresponding Green's function. This phase memory is the microscopic origin of the induced grating effect (sometimes referred to as “coherent artifact” in the literature⁶), which is a general property of coherently excited optic media with nonlinear response.⁷ The phase memory discussed here is a microscopic property of the semiconductor and is connected with the existence of individual driven e - h -pair transitions (“optically coupled states”) and their loss of phase relative to the driving field.

Carrier scattering processes provide the dominating mechanism for phase and energy relaxation of electrons and holes. The simplest analogy with atomic systems is a three-level description of transitions and their T_2 and T_1 relaxation times.⁸ Phase space filling is another factor which determines nonlinear optical properties on the ultrashort time scale. The initial build-up during the light pulse and the subsequent decay of the electron-hole-pair population is controlled by (i) the intensity of the driving light field and (ii) by the net rate of “scattering-out” due to carrier-carrier or carrier-lattice scattering. Both effects have been investigated in detail by several groups.⁹⁻¹¹

The aim of this paper is twofold. At first we point at the intrinsic phenomenon of a phase memory in both the pump- and the test-polarization fields as well as their mutual interaction. These memory effects are present as long as the pulse durations of both test and pump pulse are comparable with, or shorter than, the relevant carrier relaxation times. The second point is an analysis of quantitative experimental data on the basis of a sound many-particle theory: we illustrate how to analyze experimental data without simple phenomenological assumptions.

The first section contains a summary of relevant experimental data for GaAs at 2-eV pump photon energy. The following parts of the paper develop the basic theory on the basis of a nonequilibrium Green's function approach,^{12,13} which was investigated earlier.¹⁴⁻¹⁷ We start from first principles. Relevant scattering processes within the particle system and with the lattice are taken into account. Beside these light-matter interaction processes the interaction between pump and test fields, which was investigated only recently,¹⁸⁻²¹ is taken into account for the actual experimental arrangement. We close with a comparison of available experimental spectra with theoretical results.

II. EXPERIMENTS

Transient changes of the reflectivity after excitation with ultrashort light pulses provide important information about relaxation processes on an ultrashort time-scale. Pulse durations of 50–70 fs are now routinely generated around $\hbar\omega_0 = 2$ eV with the colliding-pulse mode-locked dye laser (CPM laser).²² Our system used intracavity dispersion compensation with a special dielectric mirror²³ and gave approximately 130 pJ energy per pulse with a spectral width of 6 nm at 620 nm central wavelength. The important chirp characteristics of our pulses were investigated with two independent methods: (i) comparison of electric field—with intensity—autocorrelation, and (ii) insertion of BK7 glass and quartz of different thickness and monitoring the changes in measured pulse duration.²⁴ Both methods gave the chirp function $c(t)$ in the electric field pulse

$$E(t) = E_0 F(t) \sin[\omega_0 + c(t)]t, \quad (2.1)$$

with

$$c(t) = \alpha t + \beta t^2 + \dots, \quad (2.2)$$

and taking for the pulse envelope function $F(t)$,

$$F(t) \sim \text{sech}(At/t_{\text{pulse}}) = 1/\cosh(At/t_{\text{pulse}}),$$

with

$$(2.3)$$

$$A = 2 \operatorname{arccosh}(\sqrt{2}) \approx 1,763.$$

Under the assumption that the leading term in the chirp function is the linear one, we varied the parameters t_{pulse} and α to fit the autocorrelation functions. Although this procedure is not unique (it depends on the functional

form of the envelope), we can give an upper limit of $\alpha = 1.5 \times 10^{-4}$ fs⁻² for the chirp of the laser pulses. As the pulses get broader with increasing thickness of glass, the laser pulses are obviously up-chirped. The field and the intensity autocorrelation function were calculated and compared with the measured one, using the parameters of Eq. (2.1), and gave very good agreement.

The magnitude of the fast transient effect (see below) in the measured change of reflectivity is expected to depend on the pulse chirp. Ippen *et al.*²⁵ showed in transmission experiments that fast transients are shifted to earlier times when the chirp is varied from positive over zero to negative values. The theoretical investigations described below show that the experimentally determined value of α can affect the calculated reflectivity spectra only to a small degree (< 5%).

Measurements of the time-dependent change of reflectivity $\Delta R/R_0$ (R_0 is the reflectivity of the unexcited sample) were performed in pump-test configuration with both pulses having the same energy and the same duration. The exciting beam was focused to a radius of 12 μm , which yields carrier densities up to 10^{18} cm⁻³. Samples of undoped GaAs bulk material of 1 mm thickness and GaAs_{0.9}P_{0.1} bulk material were used.

III. BASIC THEORY

The microscopic description of the interaction of matter with intense laser-light pulses requires a nonequilibrium Green's-function technique,^{12,13} which in recent years was successfully applied to various problems of nonlinear optics.^{14–19,26} The basic equations for the diagonal and off-diagonal elements of the one-particle propagator are

$$\begin{aligned} & \left[i\hbar \frac{\partial}{\partial t} + \varepsilon_n(-i\nabla_1) - \varepsilon_m(-i\nabla_2) \right] \tilde{G}_{<}^{nm}(1,2) \\ &= \sum_{l=v,c} \mu_{nl} E(1) \tilde{G}_{<}^{lm}(1,2) - \tilde{G}_{<}^{nl}(1,2) \mu_{lm} E(2) + (\tilde{\Sigma}_r^{nl} \tilde{G}_{<}^{lm} + \tilde{\Sigma}_{<}^{nl} \tilde{G}_a^{lm} - \tilde{G}_r^{nl} \tilde{\Sigma}_{<}^{lm} - \tilde{G}_{<}^{nl} \tilde{\Sigma}_a^{lm})_{1,2}, \end{aligned} \quad (3.1)$$

where $t = (t_1 + t_2)/2$, ε_n are band energies, and μ_{nl} are dipole transition matrix elements between valence and conduction bands. The coupling between self-energies and Green's functions is defined by

$$(\tilde{\Sigma} \tilde{G})_{1,2} = \int d^4 x_3 \tilde{\Sigma}(x_1 - x_3, (x_1 + x_3)/2) \tilde{G}(x_3 - x_2, (x_3 + x_2)/2), \quad (3.2)$$

with $x = (\mathbf{r}, t)$. Retarded (r) and advanced (a) Green's functions are determined by Dyson equations, e.g.,

$$\tilde{G}_r^{nm} = \delta_{nm} \tilde{G}_r^{0n} + \sum_l \tilde{G}_r^{0n} (\mu_{nl} E + \tilde{\Sigma}_r^{nl}) \tilde{G}_r^{lm}. \quad (3.3)$$

The occurrence of center-of-mass coordinates in (3.2) is an immediate consequence of the nonstationary external field E , which is assumed to be given as sum of a strong pump pulse E_p and a weak test pulse E_t , measuring the linear response of the excited system. As will be seen later in more detail the linear response can be calculated from the linear changes δG in the off-diagonal elements of \tilde{G} induced by the test beam. To obtain an explicit equation for δG , we introduce $\tilde{G} = G + \delta G$ and $\tilde{\Sigma} = \Sigma + \delta \Sigma$, where G is the solution of (3.1) with E replaced by E_p and $\tilde{\Sigma}$ by Σ , which contains only contributions depending on the excite pulse. Subtracting the corresponding equation for G from (3.1) and taking only linear contributions with respect to E_t in account one obtains

$$\begin{aligned}
\left[i\hbar \frac{\partial}{\partial t} + \varepsilon_n(-i\nabla_1) - \varepsilon_m(-i\nabla_2) \right] \delta G_{<}^{nm}(1,2) = & \sum_{l=v,c} \mu_{nl} E_l(1) G_{<}^{lm}(1,2) - G_{<}^{nl}(1,2) \mu_{lm} E_l(2) \\
& + \mu_{nl} E_p(1) \delta G_{<}^{lm}(1,2) - \delta G_{<}^{nl}(1,2) \mu_{lm} E_p^{(2)} \\
& + (\Sigma_r^{nl} \delta G_{<}^{lm} + \Sigma_{<}^{nl} \delta G_a^{lm} - \delta G_r^{nl} \Sigma_{<}^{lm} - \delta G_{<}^{nl} \Sigma_a^{lm})_{1,2} \\
& + (\delta \Sigma_r^{nl} G_{<}^{lm} + \delta \Sigma_{<}^{nl} G_a^{lm} - G_r^{nl} \delta \Sigma_{<}^{lm} - G_{<}^{nl} \delta \Sigma_a^{lm})_{1,2}
\end{aligned} \tag{3.4}$$

This equation takes into account finite lifetime effects on the basis of a sound many-particle theory, and does not use the concepts of longitudinal and transversal relaxation times of nonlinear optics of atomic systems, as the early theory of Bloembergen and Shen.²⁷

The system of Eq. (3.4) is valid for arbitrary pump intensities and determines the linear optical spectra of the excited system. The various contributions to (3.4) have different physical origins: The off-diagonal elements δG^{nm} , $n \neq m$, contain two contributions depending on the test beam. They describe saturation effects due to Pauli blocking, whereas the two contributions depending on the pump pulse are responsible for transient effects in the test spectra, which are caused by a coherent interaction between pump pulse and test pulse. In the limit of stationary excitation these contributions lead to light-induced gaps in the spectra, which have been discussed for some time.^{19,28-30} Other transient effects, which are described by these contributions, are (i) oscillations in transmission spectra, which occur if the test pulse precedes the pump pulse,^{20,21} (ii) the blue shift of the excitonic resonance in the case of off-resonant excitation, also called the optical Stark effect.^{18,19}

We have to distinguish between two types of the self-energy contributions to (3.4): diagonal terms describe scattering within the particle system and with phonons ($\Sigma_{<}, \Sigma_{>}$), and the renormalization of one-particle states (Σ_r, Σ_a). Off-diagonal self-energies determine the electron-hole correlation which leads to bound states. One well-known special case of (3.4) is obtained if all scattering contributions (diagonal elements of Σ) are neglected. This can be justified for off-resonant excitation. Diagonal and off-diagonal elements of δG are connected by a conservation law which makes a kinetic equation for diagonal elements redundant.^{17,19} A generalization of this conservation law to the case of nonvanishing dephasing time is straightforward.³¹ If we consider, however, real excitation processes, energy relaxation becomes crucial and an explicit treatment of the kinetic equation for diagonal elements is unavoidable as long as the pump pulse acts upon the system. This can be seen for $n = m$ in (3.4). The test and the pump pulse couple to off-diagonal elements of G and δG , respectively, in the first two contributions, which act as source contribution and thus dies out on the time scale of the pump pulse. The meaning of diagonal and off-diagonal contributions to the self-energy in (3.4) is the same as already discussed for the case $n \neq m$.

In the following we will restrict our treatment to the case of excitation far above the band edge, i.e., to excitation energies at which the bare electron-hole correlation becomes negligible and off-diagonal contributions to the

self-energy, which depend only on the bare Coulomb interaction, can be neglected (see Sec. VI).

IV. APPROXIMATION SCHEME

In order to make a numerical solution of the coupled kinetic equations for G and δG feasible, some basic approximations are necessary. From a conceptual point of view the most drastic one is the Markovian approximation in which a "local" macroscopic time scale is introduced and memory effects in the *scattering events* are neglected. Formally this implies the replacement of $(t_1 + t_3)$ and $(t_3 + t_2)$ by $(t_1 + t_2)$ in (3.2). A rigorous introduction of a local time scale can only be enforced by an infinite expansion with respect to microscopic deviations of macroscopic variables from $t = (t_1 + t_2)/2$.^{12,16} Up to now a practical evaluation of such an expansion is out of reach. One can estimate the importance of memory effects in scattering processes: Their range is determined by the lifetime of one-particle states, which is in turn determined by the scattering processes. From the known damping of one-particle states one can estimate the time scale on which memory effects will influence the relaxation process. For the density range considered here, this time is of the order of 100 fs. The Markovian approximation for scattering can be justified, if within time intervals of this order of magnitude the changes of one-particle distributions due to scattering are not too large. The rapid changes of one-particle distributions due to the excitation, as well as the interaction between pump and test pulses, are fully taken into account in our approach and lead to memory effects with a duration of the order of magnitude of 100 fs.

In the quasiparticle approximation the kinetic equations for the diagonal elements of the Green's functions can now be reduced to Boltzmann-type equations which include source contributions. The situation is more complicated for off-diagonal elements. In Fourier space G^{nm} depends on (ω, \mathbf{k}, t) . The knowledge of the frequency dependence, which is necessary in order to evaluate the coupling of G^{nm} and δG^{nm} , respectively, to the self-energies can only be obtained from the solution of the kinetic equation for $G^{nm}(\omega, \mathbf{k}, t)$. First attempts to treat such a problem numerically were reported recently²⁶ and were based on simplifying assumptions concerning the self-energies. In the present investigation the problem is tackled with the so called Shindo approximation^{32,33} which has also been discussed within the nonequilibrium Green's-function formalism.^{15,34} This approximation is often used in high excitation physics in order to treat the dynamically screened electron-hole correlation and becomes trivially exact in the stationary limit, if these

correlations are neglected. In the nonstationary case, however, the application of the Shindo approximation implies a Markovian approximation and a slowly varying amplitude approximation (SVA), as can be shown from a formal solution of (3.4) or (3.1), respectively. The SVA approximation leads to very small modifications of improved results (see Sec. V), whereas the Markovian approximation in this case is justified as long as distribution functions are small in comparison with unity. The latter is always fulfilled in the present investigation, as well as

at densities much higher than the Mott density, due to the high density of states far above the band gap.

V. KINETIC EQUATIONS FOR ONE-PARTICLE DISTRIBUTION FUNCTIONS, INDUCED DENSITIES, AND NONEQUILIBRIUM PHONONS

We apply the approximations discussed in the last section and obtain from (3.1) for $n = m$ the following equation for the one-particle distributions:

$$\begin{aligned} \hbar \frac{\partial}{\partial t} f^a(\mathbf{k}) = & -i\mu(\mathbf{k})E_p(t)\{P^{ab}(\mathbf{k}) - [P^{ab}(\mathbf{k})]^*\} - \Sigma_{<}^{aa}(\mathbf{k}, \varepsilon_a(\mathbf{k}))[1 - f^a(\mathbf{k})] + \Sigma_{>}^{aa}(\mathbf{k}, \varepsilon_a(\mathbf{k}))f^a(\mathbf{k}) \\ & - \Sigma_{<}^{ph}(\mathbf{k}, \varepsilon_a(\mathbf{k}))[1 - f^a(\mathbf{k})] + \Sigma_{>}^{ph}(\mathbf{k}, \varepsilon_a(\mathbf{k}))f^a(\mathbf{k}), \end{aligned} \quad (5.1)$$

where we have switched from the band picture to the electron-hole picture; $a \neq b$ denotes e or h , respectively. One-particle distributions and propagators are related by

$$f^a(\mathbf{k}) = -i \int \frac{d\omega}{2\pi} G_{<}^{aa}(\mathbf{k}, \omega). \quad (5.2)$$

Correspondingly we introduced the off-diagonal elements

$$P^{ab}(\mathbf{k}) = -i \int \frac{d\omega}{2\pi} G_{<}^{ab}(\mathbf{k}, \omega), \quad (5.3)$$

which obey the equation

$$\begin{aligned} \left[i\hbar \frac{\partial}{\partial t} + H(\mathbf{k}, \omega_0) - \hbar\omega_0 \right] \bar{P}^{ab}(\mathbf{k}) \\ = \mu(\mathbf{k})\bar{E}_p(t)[1 - f^a(\mathbf{k}) - f^b(\mathbf{k})] \end{aligned} \quad (5.4)$$

with

$$H(\mathbf{k}, \omega_0) = \varepsilon_a(\mathbf{k}) + \varepsilon_b(\mathbf{k}) + \bar{\Sigma}_r^{aa}(\mathbf{k}, \omega_0) + \bar{\Sigma}_r^{bb}(\mathbf{k}, \omega_0). \quad (5.5)$$

The rapidly oscillating phase factors of P and E_p have been eliminated (rotating frame) by introducing

$$\bar{P}^{ab}(\mathbf{k}) = e^{-i\omega_0 t} P^{ab}(\mathbf{k}), \quad (5.6)$$

and the corresponding definition for E_p . $\bar{\Sigma}$ denotes the effective self-energy obtained in the Shindo approximation and will be explained below, as well as the particle and phonon self-energies in (5.1) in Sec. VI. Equation (5.4) describes the coupling of the system to the excitation pulse; correspondingly one obtains from (3.4) the e - h pair density induced by the test pulse

$$\left[i\hbar \frac{\partial}{\partial t} + H(\mathbf{k}, \omega) - \hbar\omega \right] \delta\bar{P}^{ab}(\mathbf{k}) = \mu(\mathbf{k})\bar{E}_t(t)[1 - f^a(\mathbf{k}) - f^b(\mathbf{k})] - \mu(\mathbf{k})\bar{E}_p(t)e^{i(\omega_0 - \omega)t}[\delta f^a(\mathbf{k}) + \delta f^b(\mathbf{k})]. \quad (5.7)$$

$\delta\bar{P}$ is defined in correspondence to (5.6) but with ω_0 replaced by ω , the central frequency of the test pulse. The induced one-particle distributions δf occurring in (5.7) are given by

$$\begin{aligned} \hbar \frac{\partial}{\partial t} \delta f^a(\mathbf{k}) = & -i\mu(\mathbf{k})E_t(t)\{P^{ab}(\mathbf{k}) - [P^{ab}(\mathbf{k})]^*\} - i\mu(\mathbf{k})E_p(t)\{\delta P^{ab}(\mathbf{k}) - [\delta P^{ab}(\mathbf{k})]^*\} \\ & + (\Sigma_{<}^{aa} + \Sigma_{>}^{aa} + \Sigma_{<}^{ph} + \Sigma_{>}^{ph})\delta f^a(\mathbf{k}) - (\delta\Sigma_{<}^{aa} + \delta\Sigma_{<}^{ph})[1 - f^a(\mathbf{k})] + (\delta\Sigma_{>}^{aa} + \delta\Sigma_{>}^{ph})f^a(\mathbf{k}), \end{aligned} \quad (5.8)$$

where the arguments of the self-energies are the same as in (5.1). Further we have already neglected in (5.7) the very small self-energy corrections corresponding to induced renormalization and dephasing processes. The occurrence of the time derivative in (5.7) reflects that under nonstationary conditions the dependence of optical spectra on one-particle distributions is non-Markovian, as was already shown earlier.³⁵ This point has usually been overlooked in the literature, where the analysis of optical spectra on an ultrashort time scale was based on the assumption that changes in the one-particle distribution are instantaneously followed by corresponding changes in the optical spectrum.³⁶⁻³⁸ Furthermore, in the transient regime the interaction between excite and probe pulse leads to further deviations from the simple picture, which has usually been applied.

To complete the system of kinetic equations we now turn to the distribution function for nonequilibrium LO phonons. Within the present formalism the phonon propagator is in the Markovian approximation given by

$$\hbar \frac{\partial}{\partial t} D_{<}^{ph}(\mathbf{q}, \omega, t) = \frac{M^2(\mathbf{q})}{\varepsilon^2(\mathbf{q}, \omega)} [D_{>}^{ph}(\mathbf{q}, \omega, t)P_{<}(\mathbf{q}, \omega, t) - D_{<}^{ph}(\mathbf{q}, \omega, t)P_{>}(\mathbf{q}, \omega, t)], \quad (5.9)$$

with the well-known Fröhlich coupling

$$M^2(\mathbf{q}) = V(\mathbf{q}) \left[\frac{1}{\epsilon_\infty} - \frac{1}{\epsilon_0} \right] \frac{\hbar\omega_{\text{LO}}}{2} \quad (5.10)$$

and the longitudinal dielectric function $\epsilon(\mathbf{q}, \omega)$ of the excited system. If the phonon Green's function is approximated by an Einstein model and the polarization propagator is treated in random-phase approximation (RPA), one obtains after frequency integration of (5.9) the following kinetic equation for the LO-phonon distribution n :

$$\frac{\partial}{\partial t} n(\mathbf{q}) = -\frac{4\pi}{\hbar} \sum_{c=e,h} \sum_{\mathbf{k}} \frac{M^2(\mathbf{q})}{\epsilon^2(\mathbf{q}, \epsilon_{\mathbf{k}+\mathbf{q}} - \epsilon_{\mathbf{k}})} \delta(\epsilon_{\mathbf{k}+\mathbf{q}}^c - \epsilon_{\mathbf{k}}^c - \hbar\omega_{\text{LO}}) \{ [1+n(\mathbf{q})][1-f^c(\mathbf{k})]f^c(\mathbf{k}+\mathbf{q}) - n(\mathbf{q})f^c(\mathbf{k})[1-f^c(\mathbf{k}+\mathbf{q})] \}. \quad (5.11)$$

Together with certain approximations for self-energies the kinetic equations (5.1), (5.4), and (5.11) completely determine the time evolution of the system under the action of a strong laser pulse, whereas (5.7) and (5.8) describe the time-resolved response of the excited system to a weak test pulse.

VI. PARTICLE AND PHONON SELF-ENERGIES

A widely used approximation in studies of relaxation properties of highly excited semiconductors³⁶⁻⁴² is the first Born approximation for the scattering rates with a statically screened interaction. More generally the screened Hartree-Fock self-energy is given by

$$\left. \begin{array}{l} \Sigma_{<}^{\text{SHF}}(1,2) \\ \Sigma_{>}^{\text{SHF}}(1,2) \end{array} \right\} = i\hbar \times \left\{ \begin{array}{l} W_{<}(2,1)G_{<}(1,2) \\ W_{>}(2,1)G_{>}(1,2) \end{array} \right\}, \quad (6.1)$$

where the propagator of the longitudinal interaction obeys the relation

$$W_{>}(1,2) = \int d3 \int d4 W_r(1,3)P_{>}(3,4)W_a(4,2). \quad (6.2)$$

Using P in the RPA and taking also into account the exchange diagram corresponding to (6.1), the total particle self-energy reads

$$\Sigma_{<}^{aa}(1,2) = 2\hbar^2 \int d3 \int d4 \left\{ \sum_c W_r(3,1)G_{>}^{cc}(3,4)G_{<}^{cc}(4,3)W_a(2,4)G_{<}^{aa}(1,2) - \frac{1}{2} W_r(3,1)G_{>}^{cc}(1,4)G_{<}^{cc}(4,3)W_a(2,4)G_{<}^{aa}(1,2) \right\}. \quad (6.3)$$

Equation (6.3) can be evaluated by using a quasiparticle representation for the particle propagators and again a Markovian approximation. One obtains

$$\Sigma_{<}^{aa}(\mathbf{k}, \omega, t) = \sum_{c=e,h} \sum_{\mathbf{k}_1, \mathbf{k}_2} \delta(\hbar\omega + \epsilon_{\mathbf{k}_1}^c - \epsilon_{\mathbf{k}-\mathbf{k}_2}^a - \epsilon_{\mathbf{k}_1+\mathbf{k}_2}^c) [2|W_r(\hbar\omega - \epsilon_{\mathbf{k}-\mathbf{k}_2}^a, \mathbf{k}_2)|^2 - \delta_{ca} W_r(\hbar\omega - \epsilon_{\mathbf{k}-\mathbf{k}_2}^a, \mathbf{k}_2) \times W_a(\hbar\omega - \epsilon_{\mathbf{k}_1+\mathbf{k}_2-\mathbf{k}}^a, \mathbf{k}_1 + \mathbf{k}_2 - \mathbf{k})] [1 - f^c(\epsilon_{\mathbf{k}_1}^c)] f^a(\epsilon_{\mathbf{k}-\mathbf{k}_2}^a) f^c(\epsilon_{\mathbf{k}_1+\mathbf{k}_2}^a). \quad (6.4)$$

The corresponding $\Sigma_{>}$ is obtained by interchanging f and $(1-f)$ in (6.4). In the derivation of (6.4) renormalization effects on the time scale of the excitation pulse, which would lead to light-induced modifications in the one-particle spectrum, are neglected for the following reason: Sharp light-induced gaps²⁸⁻³⁰ do not occur if the finite spectral width of the driving pulse is considered. Nevertheless, the one-particle density of states can be modified considerably for high-field intensities. The effect, however, is negligible, as long as the Rabi frequency is small in comparison with the spectral width of the pulse.

The scattering contribution of LO phonons is given in analogy to (5.11) by

$$\Sigma_{<}^{ph}(1-f^e) - \Sigma_{>}^{ph}f^e = \frac{2\pi}{\hbar} \sum_{\mathbf{q}} \frac{M^2(\mathbf{q})}{\epsilon^2(\mathbf{q}, \epsilon_{\mathbf{k}+\mathbf{q}} - \epsilon_{\mathbf{k}})} \delta(\epsilon_{\mathbf{k}+\mathbf{q}}^c - \epsilon_{\mathbf{k}}^c - \hbar\omega_{\text{LO}}) \times \{ [1+n(\mathbf{q})][1-f^c(\mathbf{k})]f^c(\mathbf{k}+\mathbf{q}) - n(\mathbf{q})f^c(\mathbf{k})[1-f^c(\mathbf{k}+\mathbf{q})] \}. \quad (6.5)$$

Now we turn to the discussion of the effective self-energies, which enter the kinetic equations for the off-diagonal elements (5.4) and (5.7). The first contribution is the well-known static exchange self-energy

$$\Sigma_{\text{exc}}^{aa}(\mathbf{k}) = - \sum_{\mathbf{k}'} V(\mathbf{k}-\mathbf{k}') f^a(\epsilon_{\mathbf{k}'}). \quad (6.6)$$

It causes a nearly \mathbf{k} -independent shift of electron and hole bands to lower energies.

The second contribution can be calculated from the dynamical electron-hole interaction, which occurs in the self-energy contributions in (3.4). As was shown in detail^{15,34} using the screened Hartree-Fock scheme and the already discussed Shindo approximation, the dynamical contribution to the electron-hole interaction can be cast into the form

$$\begin{aligned} \Delta w(\omega, \mathbf{k}, \mathbf{k}') = & [1 - f^e(\mathbf{k}') - f^h(\mathbf{k}')]^{-1} \int \frac{d\Omega}{2\pi} \int \frac{d\Omega'}{2\pi} \\ & \times (-G^c_{<} \Delta w_a G^c_{<} - G^c_{>} w_{<} G^c_{>} + G^c_{<} w_{>} G^c_{>} \\ & - G^v_{<} \Delta w_r G^v_{<} - G^v_a w_{<} G^v_{<} + G^v_{<} w_{>} G^v_{>} + G^c_{<} \Delta w_a G^v_{<} + G^c_{>} w_{<} G^v_{<} - G^c_{<} w_{>} G^v_a \\ & + G^v_{<} \Delta w_r G^c_{<} + G^v_a w_{<} G^c_{<} - G^v_{<} w_{>} G^c_{>}), \end{aligned} \quad (6.7)$$

where we have used the abbreviations $G^c = G^c(\Omega + \Omega', \mathbf{k} + \mathbf{k}')$, $G^v = G^v(\Omega + \Omega' - \omega, \mathbf{k} + \mathbf{k}')$, $G^c_{>} = G^c(\Omega', \mathbf{k}')$, $G^v_{>} = G^v(\Omega' - \omega, \mathbf{k}')$, $w = w(\Omega, \mathbf{k})$, and $\Delta w = w - v$. To obtain insight into the physical processes determining this effective interaction it is advantageous to consider the imaginary part of (6.7), which is given by

$$\text{Im}\{\Delta w(\omega, \mathbf{k}, \mathbf{k}')\} = [1 - f^e(\mathbf{k}') - f^h(\mathbf{k}')]^{-1} \int \frac{d\Omega}{2\pi} \int \frac{d\Omega'}{2\pi} \sum_{a=c,v} (G^a_{<} w_{>} G^c_{>} - G^a_{>} w_{<} G^c_{<} - G^a_{<} w_{>} G^v_{>} + G^a_{>} w_{<} G^v_{<}), \quad (6.8)$$

with $w_{<}$ and $w_{>}$, respectively, defined by (6.2).

As a result the imaginary part of the dynamical contributions to the effective self-energies in (5.4) is obtained

$$\text{Im}\{\overline{\Delta\Sigma}(\omega, \mathbf{k})\} = \sum_{\mathbf{k}'} [\text{Im}\{\Delta w(\omega, \mathbf{k}', \mathbf{k})\} - \text{Im}\{\Delta w(\omega, \mathbf{k} - \mathbf{k}', \mathbf{k}')\}] P(\mathbf{k}')/P(\mathbf{k}) \quad (6.9)$$

and the real part of $\overline{\Delta\Sigma}$ can be calculated from the Hilbert transformation of (6.9). The corresponding contribution in (5.7) is obtained from (6.9) with P replaced by δP .

The second contribution on the right-hand side of (6.9) corresponds to vertex corrections. Their inclusion is essential for the following reason: If only the pure self-energy contribution to (6.9) would be considered, one would obtain the unphysical result that in the limit of vanishing density (respectively, vanishing screening) the damping would approach a finite value. This is an immediate consequence of the singularity of the bare Coulomb interaction. As can be seen from (6.9) together with (6.8), the vertex corrections cancel this singularity exactly. They guarantee that $\text{Im}\{\overline{\Delta\Sigma}\}$ vanishes with vanishing density and cause that electronic dephasing processes are necessarily off diagonal in k space. Beside this technical detail a comparison of (6.8) with (5.1) and (6.1) demonstrates that the processes governing the effective electronic dephasing time of the off-diagonal elements are the same which determine the relaxation of one-particle distributions. Although this point is intuitively clear, up to now only phenomenological approaches have been applied. The result (6.9) represents the first microscopic approach to dephasing times in highly excited semiconductors.

To complete this section, we explain the approximation used in actual calculations for the screened interaction. An approximation scheme, fully consistent with the Born approximation already used for the scattering cross sections in (6.1), requires the calculation of the RPA dielectric function under nonequilibrium conditions. Unfortunately the Pade approximant technique applied,³⁴ which allows a full RPA calculation of screening proper-

ties in quasiequilibrium cannot be applied to the case of nonmonotonous one-particle distributions. Therefore, we restrict ourselves to the common plasmon approximation, in which the dielectric function is given by

$$\epsilon(\omega, \mathbf{q}) = 1 - \frac{\omega_{pl}^2}{(\omega + i\Gamma)^2 + \omega_{pl}^2 - \omega^2(\mathbf{q})}, \quad (6.10)$$

with the plasmon dispersion defined by

$$\hbar^2 \omega^2(\mathbf{q}) = \hbar^2 \omega_{pl}^2 \left[1 + \frac{q^2}{\kappa^2} \right] + \frac{1}{4} [\epsilon_e(\mathbf{q}) + \epsilon_h(\mathbf{q})]^2 \quad (6.11)$$

and the screening vector

$$\kappa = -8\pi e^2 \sum_{\mathbf{k}, q=e,h} \frac{\partial f_a[\epsilon_a(\mathbf{k})]}{\partial \epsilon_a(\mathbf{k})}. \quad (6.12)$$

The explicit consideration of the coupling between plasmons and phonons,⁴³ which results from the level crossing of the plasma dispersion with the LO-phonon energy, can be neglected for the densities under consideration. Divergence problems occurring in principle in (6.5) are avoided by a small numerical damping Γ in (6.10).

VII. CALCULATION OF TRANSIENT REFLECTIVITY SPECTRA

The theory outlined in the last sections has led to a closed system of equations determining one-particle distributions and transition amplitudes (off-diagonal elements) induced by the excitation pulse. Energy relaxation of diagonal and dephasing of off-diagonal elements of the induced density are treated on an equal footing. Now

the question of measurable quantities has to be discussed. The concept of Fresnel's formulas for the reflectivity at an interface under stationary conditions (i.e., cw light) has to be critically tested in the case of ultrashort transients discussed here. The effect of scattering of the pump beam into the reflected test beam has been treated in detail by Eichler,⁷ and will not be discussed here. From Maxwell's equations and the usual boundary conditions one obtains for the reflected field

$$E_r(t) = R_0 E_i(t) + \frac{\Delta \delta P^{eh}(t)}{n_0(n_0 + 1)^2} + O\left[\frac{d\Delta \delta P^{eh}(t)}{dt}\right], \quad (7.1)$$

where n_0 denotes the complex index of refraction of the unexcited system, and E_r has been linearized with respect to $\Delta \delta P^{eh} = \delta P^{eh}[E_p] - \delta P^{eh}[E_p = 0]$. Corrections to the first two terms of the right-hand side of (7.1), which become important for ultrashort pulses and very high densities, have been investigated.⁴⁴ For pulse durations of the order of about 100 fs and densities of the order of $n = 0.1 n_b^{-3}$ these corrections are less than 1%. Recent investigations at higher densities⁴⁵ seem to indicate that these corrections indeed become important. In our present investigation we concentrate ourselves on smaller densities, so that these corrections are small in comparison with the dominating change of reflectivity spectra. Thus we obtain from (7.1) for the relative change of the reflection coefficient

$$\Delta R(\omega, \tau) = 2 \operatorname{Re} \left[\frac{NR_0^*}{n_0(n_0 + 1)^2} \int dt E_i^*(t) \Delta \delta P^{eh}(\omega, t - \tau) \right], \quad (7.2)$$

with the normalization constant defined by

$$N = \left[\int dt |E_i(t)|^2 \right]^{-1}. \quad (7.3)$$

Equation (7.2) is valid for a photodetector which integrates the reflected field without preceding spectral filtering.³¹ Note that the test field implicitly depends on its central frequency and the time delay τ with respect to the excite pulse.

VIII. RESULTS AND DISCUSSION

Figure 1 shows the measured time-resolved change of test-beam reflectivity $\Delta R/R_0$. The fast increase of the reflectivity follows closely the time dependence of the exciting laser pulses and reaches its maximum value with a time delay of $\tau = +40 \pm 30$ fs of the test pulse. Two time scales are obviously relevant for the decrease of the measured signal. First a fast component of the order of the pulse duration, followed by a slower decay, which depends on the excitation density. The slow relaxation time is 8 ps for an excitation density of 10^{18} cm^{-3} and increases to 12 ps at excitation density 10^{17} cm^{-3} . The slow decay is caused by carrier scattering within the particle system and by carrier-phonon scattering, both leading to a quasiequilibrium distribution. We emphasize that the shape of the spike is (within the accuracy of the measurements) independent of the excitation density.

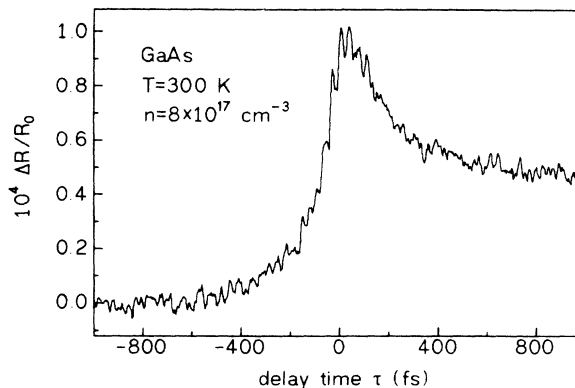


FIG. 1. Measured time-dependent change of test-beam reflectivity for GaAs.

Figure 2 shows the maximum value of the change in reflectivity $\Delta R/R_0$ for different excitation densities. The absolute value of $\Delta R/R_0$ grows linearly with the excitation intensity up to a density of 10^{18} cm^{-3} . For higher densities $n > 10^{18} \text{ cm}^{-3}$ deviations from this linear behavior correspond to the onset of saturation due to phase space filling.

To analyze the experimental data on the basis of the theory outlined in the preceding sections, it is necessary to solve the kinetic equations obtained in Sec. V together with (6.4)–(6.6) and (6.9) for a realistic model of the band structure of GaAs. A corresponding model should involve light-, heavy-, and split-off hole bands, and a suitable parameterization of electron bands including non-parabolicity, multivalley degeneracy, and warping. First attempts to include some of these band-structure effects in Monte Carlo simulations^{42,46} have been reported recently. A full description, however, of the various scattering processes within and between different bands and valleys is out of reach at the moment. Therefore we focus our interest on a two-band model, describing two

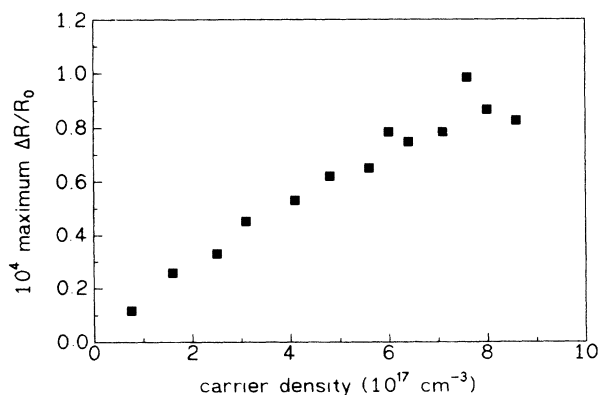


FIG. 2. Carrier-density dependence of the peak value of $\Delta R/R_0$ (see text).

parabolic bands and only one transition-matrix element, the \mathbf{k} dependence of which is obtained from $\mathbf{k}\cdot\mathbf{p}$ perturbation theory.⁴⁷ Numerical calculations are performed using the same methods applied earlier.^{34,35} Parameters used for the calculations are the following:

$$\begin{aligned} E_G &= 1.519 \text{ eV} & m_h &= 0.48m_0 \\ |P_{CV}|^2/2m_0 &= 7.4 \text{ eV} & m_e &= 0.065m_0 \\ E_b &= 4.2 \text{ meV} & \epsilon_0 &= 12.3 \\ r_b &= 124 \text{ \AA} & \epsilon_\infty &= 10.9 \end{aligned}$$

The calculated results of the relative change of reflectivity are plotted in Fig. 3. The comparison with the experimental data for larger times ($\tau > 500$ fs) shows good agreement. The absolute theoretical value is too low by a factor of 2. The slope for larger times is two times smaller than the experimental result. Apart from the influence of band-structure effects, i.e., the broadening of initial distributions due to warping, a possible explanation for this difference is the carrier diffusion out of the test volume, which is not taken into account in the numerical calculations. The fast component is less pronounced than in the measured curve, nevertheless the decrease caused by this fast component stops at a relative higher value of $\Delta R/R_0$ than in the experiment. It is important to emphasize, therefore, that the theory explains a fast component in the change of reflectivity without the consideration of the intervalley scattering from the Γ valley to the X and L valleys. The scattering times for these processes are 180 fs for $\Gamma \rightarrow X$ and 540 fs for $\Gamma \rightarrow L$ scattering.⁴⁸ A commonly used assumption to determine these time constants from transient reflectivity or transmission measurements^{49,50} is the identification of a scattering time with the mean duration of the fast component. This, however, is not justified if several different physical processes contribute to the rapid decay. Our theoretical analyses shows, that even without intervalley scattering, three distinct fast processes are involved on a time scale up to 150 fs. (i) The interaction between pump and test beam [compare Eqs. (5.7) and (5.8)] which is restricted to the duration of the excitation process, (ii) LO-phonon scattering of carriers, and (iii) the rapid relaxa-

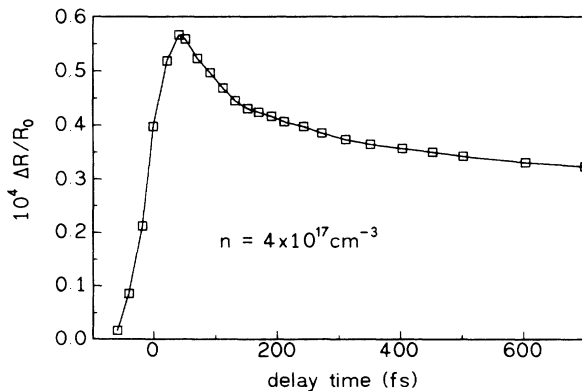


FIG. 3. Calculated time-dependent change in reflectivity.

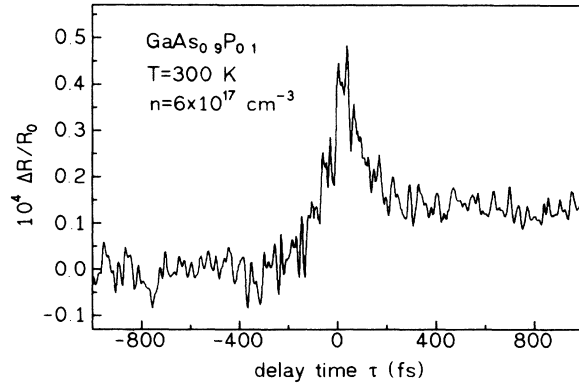


FIG. 4. Measured time-dependent change in reflectivity for $\text{GaAs}_{0.9}\text{P}_{0.1}$.

tion of the hole distribution. The presence of any further fast process would lead to a relative increase of the fast component. The good agreement between theory and experiment indicates that intervalley scattering is not the dominant scattering process under the chosen experimental conditions. This is confirmed by further measure-

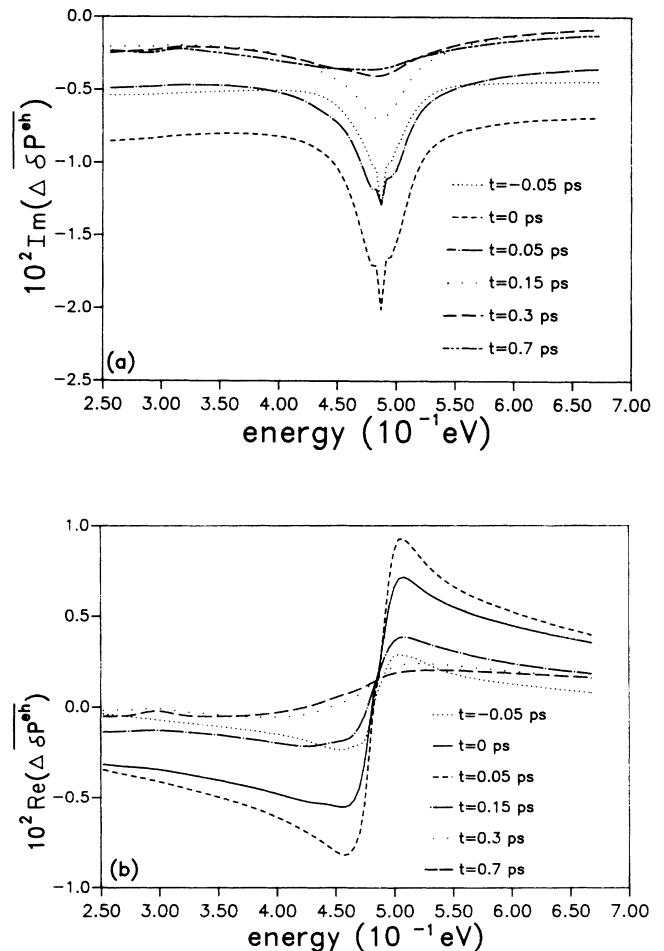


FIG. 5. Energy dependence of the difference of the (a) imaginary and (b) real part of $\Delta\delta P^{eh}$ for various delay times between pump pulse and test pulse.

ments which we performed in a GaAs_{0.9}P_{0.1} sample, where the $\Gamma \rightarrow X$ transfer is not allowed.⁵¹ The same behavior of the time evolution of $\Delta R/R_0$ was found after the sample was excited by the laser pulse (see Fig. 4).

The numerical results are now discussed in more detail by insertion of the real and imaginary part of the time-averaged-induced density entering (7.2). In Fig. 5 the time averaged difference spectra, $\Delta\delta P^{eh}$, occurring in (7.2), are shown for various delay times τ between the pump pulse and the test pulse at the density $n = 4 \times 10^{17} \text{ cm}^{-3}$. The structure of the spectral hole around the excitation energy, shown in Fig. 5(a), can be understood in principle if the interaction contributions between excite pulse and probe pulse [second term on the right-hand side of (5.7)] are considered in the limit of vanishing relaxation and dephasing. In this limit δn^{aa} can be obtained from the already mentioned conservation rule, leading to

$$\delta n^{aa}(\mathbf{k}, t) = P^{ab}(\mathbf{k}, t) \delta P^{ba}(\mathbf{k}, t) + P^{ba}(\mathbf{k}, t) \delta P^{ab}(\mathbf{k}, t). \quad (8.1)$$

Thus δn contains the product of the real and the imaginary parts of P and δP , respectively. These two contributions cause an energetically localized and an extended contribution to the spectral hole. The duration of this effect is limited by the pulse duration, if it is short in comparison with the duration of dephasing processes, or by a mean dephasing time in the opposite case. The Pauli blocking in Eq. (5.7) causes the third contribution to the spectral hole, which is present as long as the one-particle distributions peaks in the vicinity of the excitation energy. Apart from the spike at the excitation energy, similar hole-burning effects are well known in saturation spectroscopy of atomic systems.⁵¹ For delay times longer than ≈ 120 fs only Pauli blocking contributes to the spectral hole burning. For larger times the hole contribution becomes considerably broadened and is shifted to lower energies.

The hole in $\text{Im}\{\overline{\Delta\delta P^{eh}}\}$ leads to an immediate decrease of the absorption observed in transmission experiments.^{25,49,50} The change in reflectivity $\Delta R/R_0$, however, is dominated by the temporal change of $\text{Re}\{\Delta\delta P^{eh}\}$. Whether the change in $\Delta R/R_0$ at the excitation energy is larger or smaller than zero depends crucially on the asymmetry of the one-particle distributions with respect to the excitation energy. If the first moments of the distribution functions are smaller than the excess energies with respect to the band minima, the zeros of $\text{Re}\{\Delta\delta P^{eh}\}$, shown in Fig. 5(b), are shifted to energies smaller than the excitation energy $\hbar\omega_0$. The immediate consequence of this shift is an increase of the reflectivity, i.e., $\Delta R/R_0 > 0$ at $\hbar\omega_0$.

The calculated energy-dependent distribution functions for different delay times are plotted for the electrons in Fig. 6 and for the holes in Fig. 7. For the holes the phonon sideband becomes significant already at $t = -15$ fs. Carrier-carrier scattering causes a fast broadening of the distribution function. After 400 fs the holes are practically thermalized and can be described by a thermal distribution.

The electron distribution function is much broader

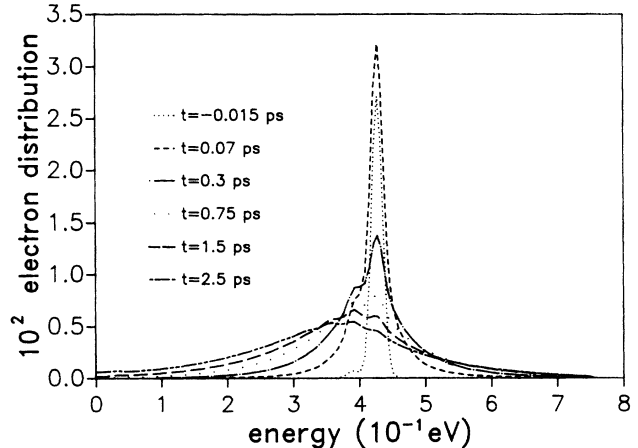


FIG. 6. Energy-dependent electron distribution function for various delay times between pump pulse and test pulse.

than the distribution function for the holes. This is due to the smaller effective mass of the conduction band compared with the valence-band mass. Thus for small times phonon sidebands appear only as structures within the energetical range of the distribution generated by the pulse. These structures are effectively smeared out by the Coulomb scattering of carriers. For later times the distribution shows a significant broadening and a shift of the energy peak to smaller energies. But even after 2.5 ps the electrons are not thermalized. It should be noted that within the present treatment of the Coulomb scattering cross sections the relaxation processes are faster by nearly a factor of 2 in comparison with a statically screened interaction.⁵² This surprisingly long duration of the relaxation process is confirmed qualitatively by recent transmission measurements.^{49,50}

IX. SUMMARY

On the basis of a microscopic nonequilibrium theory of energy relaxation and dephasing processes of e - h pairs we

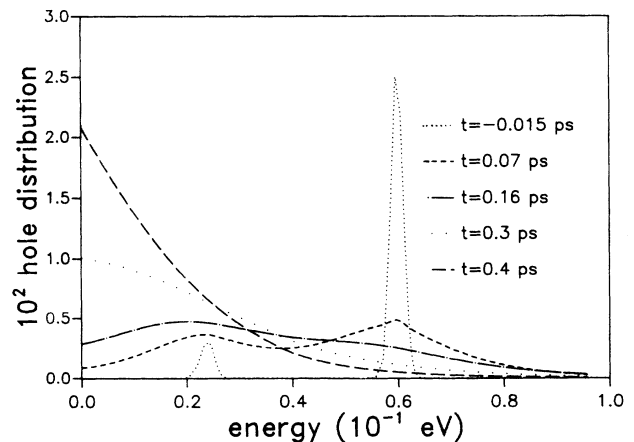


FIG. 7. Energy-dependent hole distribution function for various delay times between pump pulse and test pulse.

have shown that on an ultrashort time scale of the order of 100 fs the mutual interaction between pump and test beam leads to a significant modification of the spectral hole caused by Pauli blocking. Together with the dominant relaxation processes due to LO-phonon and hole-

hole scattering this effect leads to a spike in transient reflectivity and transmission spectra. Our theoretical description of the shape and magnitude of nonlinear reflectivity spectra agrees very well with experimental results.

- ¹W. H. Knox, IEEE J. Quantum Electron. **QE-24**, 388 (1988).
- ²J. Appel, Phys. Rev. **122**, 1760 (1961); **125**, 1815 (1962). M. Asche and O. G. Sarbei, Phys. Status Solidi B **126**, 607 (1984).
- ³E. M. Conwell, *High Field Transport in Semiconductors*, Vol. 9 of *Solid State Physics* (Academic, New York, 1967).
- ⁴M. Born and R. Oppenheimer, Ann. Phys. (NY) **84**, 457 (1927).
- ⁵D. H. Auston, Appl. Phys. Lett. **43**, 713 (1983).
- ⁶E. P. Ippen and C. V. Shank, in *Ultrashort Light Pulses*, Vol. 18 of *Topics in Applied Physics*, edited by S. L. Shapiro (Springer, Berlin, 1977), p. 108.
- ⁷H. J. Eichler, P. Günter, and D. W. Pohl, *Laser-Induced Dynamic Gratings* (Springer, Berlin, 1986).
- ⁸Y. R. Shen, *The Principles of Nonlinear Optics* (Wiley, New York, 1984).
- ⁹J. L. Oudar, A. Migus, D. Hulin, G. Grillon, J. Etchepare, and A. Antonetti, Phys. Rev. Lett. **53**, 384 (1984).
- ¹⁰W. Z. Lin, R. W. Schoenlein, J. G. Fujimoto, and E. P. Ippen, IEEE J. Quantum Electron **QE-24**, 267 (1988).
- ¹¹W. H. Knox, D. S. Chemla, G. Livescu, J. E. Cunningham, and J. E. Henry, Phys. Rev. Lett. **61**, 1290 (1988).
- ¹²L. P. Kadanoff and G. Baym, *Quantum Statistical Mechanics* (Benjamin, New York, 1962).
- ¹³L. V. Keldysh, Zh. Eksp. Teor. Fiz. **47**, 1515 (1964) [Sov. Phys.—JETP **20**, 1018 (1965)].
- ¹⁴H. Haug, in *Optical Nonlinearities and Instabilities in Semiconductors*, edited by H. Haug (Academic, New York, 1988); W. Schäfer, *ibid.* p. 135.
- ¹⁵W. Schäfer and J. Treusch, Z. Phys. B **63**, 407 (1986).
- ¹⁶K. Henneberger, V. May, Physica A (Amsterdam) **138**, 537 (1986).
- ¹⁷W. Schäfer, in *Festkörperprobleme (Advances in Solid State Physics)*, edited by U. Rössler (Vieweg, Braunschweig, 1988), Vol. 28, p. 63.
- ¹⁸S. Schmitt-Rink and D. S. Chemla, Phys. Rev. Lett. **57**, 2752 (1986).
- ¹⁹S. Schmitt-Rink, D. S. Chemla, and H. Haug, Phys. Rev. B **37**, 941 (1988).
- ²⁰B. Fluegel, N. Peyghambarian, G. Olbright, M. Lindberg, S. W. Koch, M. Joffre, D. Hulin, A. Migus, and A. Antonetti, Phys. Rev. Lett. **59**, 2588 (1987).
- ²¹M. Lindberg and S. Koch, Phys. Rev. B **38**, 7607 (1988).
- ²²R. L. Fork, B. I. Greene, and C. V. Shank, Appl. Phys. Lett. **38**, 671 (1981).
- ²³J. Kuhl and J. Heppner, IEEE J. Quantum Electron. **QE-22**, 182 (1986).
- ²⁴J. C. M. Diels, J. J. Fontaine, I. C. McMichael, and F. Simoni, Appl. Optics **24**, 1270 (1985).
- ²⁵W. Z. Lin, J. G. Fujimoto, and E. P. Ippen, *Ultrafast Phenomena*, edited by G. R. Flemming and A. E. Siegman (Springer, Berlin, 1986), Vol. 5.
- ²⁶M. Hartmann, R. Zimmermann, and A. Stolz, Phys. Status Solidi B **146**, 357 (1988).
- ²⁷N. Bloembergen and Y. R. Shen, Phys. Rev. A **37**, 139 (1964).
- ²⁸V. F. Elesin, Zh. Eksp. Teor. Fiz. **59**, 602 (1970).
- ²⁹T. Harbich and G. Mahler, Phys. Status Solidi B **117**, 653 (1983).
- ³⁰K. Henneberger and K. H. Kühn, Physica A **150**, 439 (1988).
- ³¹R. Zimmermann and M. Hartmann, Phys. Status Solidi B **150**, 379 (1988).
- ³²K. Shindo, J. Phys. Soc. Jpn. **29**, 287 (1970).
- ³³R. Zimmermann, K. Kilimann, W. Kraeft, D. Kremp, and G. Röpke, Phys. Status Solidi B **90**, 175 (1978).
- ³⁴W. Schäfer, R. Binder, and K. H. Schuldt, Z. Phys. B **70**, 145 (1988).
- ³⁵W. Schäfer, R. Binder, and K. H. Schuldt, J. Lumin. **38**, 282 (1987).
- ³⁶P. Lugli and S. M. Goodnick, Appl. Phys. Lett. **51**, 584 (1983).
- ³⁷S. M. Goodnick and P. Lugli, Phys. Rev. B **37**, 2578 (1988).
- ³⁸J. Collet and T. Amand, Physica B+C **134B**, 394 (1985).
- ³⁹J. Collet, T. Amand, and M. Pugno, Phys. Lett. A **96**, 368 (1983).
- ⁴⁰J. Zimmermann, P. Lugli, and D. K. Ferry, Solid State Electron. **12**, 233 (1983).
- ⁴¹J. Collet and T. Amand, J. Phys. Chem. Solids **47**, 153 (1986).
- ⁴²M. A. Osman and D. K. Ferry, Phys. Rev. B **36**, 6018 (1987).
- ⁴³H. Sato and Y. Hori, Phys. Rev. B **36**, 6033 (1987).
- ⁴⁴F. Gawehn and M. Schubert in *Ultrafast Phenomena*, edited by E. Klose and B. Wilhelmi (Teubner, Leipzig, 1986), p. 44.
- ⁴⁵H. Kurz, W. Kuett, K. Seibert, and M. Strahnen, Solid State Electron. **31**, 447 (1988).
- ⁴⁶C. J. Stanton, D. W. Bailey, K. Hess, and Y. C. Cheng, Phys. Rev. B **37**, 6575 (1987).
- ⁴⁷E. O. Kane, J. Phys. Chem. Solids **1**, 249 (1957).
- ⁴⁸R. G. Ulbrich, J. A. Kash, and J. C. Tsang, Phys. Rev. Lett. **62**, 949 (1989).
- ⁴⁹W. Z. Lin, J. G. Fujimoto, and E. P. Ippen, Appl. Phys. Lett. **51**, 161 (1987).
- ⁵⁰W. Z. Lin, R. W. Schoenlein, M. J. La Gasse, B. Zysset, E. P. Ippen, and J. G. Fujimoto, in *Ultrafast Phenomena*, edited by T. Yajima, K. Yoshihara, C. B. Harris, and S. Shionoya (Springer, Berlin, 1988), Vol. 6, p. 210.
- ⁵¹A.-B. Chen and A. Sher, Phys. Rev. B **23**, 5360 (1981).
- ⁵²V. S. Letokhov and V. P. Chebotayer, *Nonlinear Laser Spectroscopy*, Chap. 2 (Springer, Heidelberg, 1977).